NeuroImage: Clinical 21 (2019) 101619

Contents lists available at ScienceDirect

NeuroImage: Clinical

journal homepage: www.elsevier.com/locate/ynicl

Abnormal topological organization of structural covariance networks in amyotrophic lateral sclerosis

Yuanchao Zhang[a], Ting Qiu[a], Xinru Yuan[a], Jinlei Zhang[a], Yue Wang[a], Na Zhang[b], Chaoyang Zhou[c], Chunxia Luo[d], Jiuquan Zhang[e,f,*]

[a] Key Laboratory for NeuroInformation of Ministry of Education, School of Life Science and Technology, University of Electronic Science and Technology of China, Chengdu 610054, PR China
[b] School of Mathematical Sciences, University of Jinan, Jinan 250022, Shandong Province, PR China
[c] Department of Radiology, Southwest Hospital, Third Military Medical University, Chongqing 400038, PR China
[d] Department of Neurology, Southwest Hospital, Third Military Medical University, Chongqing 400038, PR China
[e] Department of Radiology, Chongqing University Cancer Hospital, Chongqing Cancer Institute, Chongqing Cancer Hospital, Chongqing 400030, PR China
[f] Key Laboratory for Biorheological Science and Technology of Ministry of Education (Chongqing University), Chongqing University Cancer Hospital, Chongqing Cancer Institute, Chongqing Cancer Hospital, Chongqing 400044, PR China

ARTICLE INFO

Keywords:
Amyotrophic lateral sclerosis
Structural covariance network
Gray matter volume
Small-world
Modularity

ABSTRACT

Neuroimaging studies of patients with amyotrophic lateral sclerosis (ALS) have shown widespread alterations in structure, function, and connectivity in both motor and non-motor brain regions, suggesting multi-systemic neurobiological abnormalities that might impact large-scale brain networks. Here, we examined the alterations in the topological organization of structural covariance networks of ALS patients ($N = 60$) compared with normal controls ($N = 60$). We found that structural covariance networks of ALS patients showed a consistent rearrangement towards a regularized architecture evidenced by increased path length, clustering coefficient, small-world index, and modularity, as well as decreased global efficiency, suggesting inefficient global integration and increased local segregation. Locally, ALS patients showed decreased nodal degree and betweenness in the gyrus rectus and/or Heschl's gyrus, and increased betweenness in the supplementary motor area, triangular part of the inferior frontal gyrus, supramarginal gyrus and posterior cingulate cortex. In addition, we identified a different number and distribution of hubs in ALS patients, showing more frontal and subcortical hubs than in normal controls. In conclusion, we reveal abnormal topological organization of structural covariance networks in ALS patients, and provide network-level evidence for the concept that ALS is a multisystem disorder with a cerebral involvement extending beyond the motor areas.

1. Introduction

Amyotrophic lateral sclerosis (ALS) is an idiopathic and fatal neurodegenerative disease characterized by a progressive degeneration of both upper and lower motor neurons, leading to limb paralysis, dysarthria, dysphagia, and respiratory failure (Kiernan et al., 2011; Swinnen and Robberecht, 2014). In addition to motor system pathology, ALS is also associated with varying degrees of extra-motor brain degeneration, affecting behavior, language and cognitive functions (Goldstein and Abrahams, 2013; Murphy et al., 2007; Tsermentseli et al., 2012). Indeed, up to 50% of ALS patients show cognitive and/or behavioral changes, while 10–15% exhibit more severe impairment and meet criteria for frontotemporal dementia (FTD) (Montuschi et al., 2015). Furthermore, ALS shares a common neuropathology with FTD that is characterized by the deposition of TAR DNA-binding protein 43 (TDP-43) (Neumann et al., 2006; Riku et al., 2014).

Neuroimaging studies of ALS patients have documented aberrant brain structure and function for regions underlying motor and non-motor functioning. Structural MRI studies demonstrated reduced gray

Abbreviations: ALS, Amyotrophic lateral sclerosis; FTD, frontotemporal dementia; TDP-43, TAR DNA-binding protein 43; DTI, diffusion tensor imaging; ALSFRS-R, ALS Functional Rating Scale-Revised; GM, gray matter; WM, white matter; ROI, regions of interest; AUC, area under the curve; GR, gyrus rectus; HG, Heschl's gyrus; PCC, posterior cingulate cortex; IFG, inferior frontal gyrus; SMA, supplementary motor area; SMG, supramarginal gyrus

* Corresponding author at: Department of Radiology, Chongqing University Cancer Hospital, Chongqing Cancer Institute, Chongqing Cancer Hospital, Chongqing 400030, PR China.
E-mail address: zhangjq_radiol@foxmail.com (J. Zhang).

https://doi.org/10.1016/j.nicl.2018.101619
Received 23 May 2018; Received in revised form 3 November 2018; Accepted 29 November 2018
Available online 30 November 2018

matter volume and cortical thickness in both motor and extra-motor regions, involving the frontal (Bede et al., 2013; Menke et al., 2014; Verstraete et al., 2012; Walhout et al., 2015), temporal (Ash et al., 2015; Chang et al., 2005; Senda et al., 2017; Thivard et al., 2007), parietal (Ash et al., 2015; Cosottini et al., 2012; Kim et al., 2017; Thivard et al., 2007; Thorns et al., 2013), and limbic cortices (D'Ambrosio et al., 2014; Shen et al., 2016; Terada et al., 2017; Tsujimoto et al., 2011). Diffusion tensor imaging (DTI) studies consistently reported abnormal diffusion parameters in corticospinal tracts (Cosottini et al., 2005; Iwata et al., 2011; Menke et al., 2016; Muller et al., 2016; Thivard et al., 2007) and corpus callosum (Filippini et al., 2010; Iwata et al., 2011; Menke et al., 2016; Zhang et al., 2017), as well as extra-motor regions, especially the frontotemporal areas (Lule et al., 2010; Muller et al., 2016; Senda et al., 2009; Tsujimoto et al., 2011). Resting-state fMRI studies reported both increased (Agosta et al., 2011; Douaud et al., 2011; Heimrath et al., 2014; Menke et al., 2016) and decreased (Agosta et al., 2013a; Jelsone-Swain et al., 2010; Mohammadi et al., 2009; Tedeschi et al., 2012; Zhang et al., 2017) functional connectivity in motor and extra-motor brain networks. This body of evidence suggests that ALS is associated with multi-systemic neurobiological abnormalities that might impact large-scale brain networks.

Graph theory provides a powerful tool for characterizing the topological organization of large-scale brain networks. Using this method, previous studies have demonstrated that brain networks of healthy individuals have an economical small-world topology and a modular organization (Achard et al., 2006; Chen et al., 2008; Fan et al., 2011; He et al., 2007; Meunier et al., 2009). The small-world architecture is characterized by a high degree of local clustering and short path length linking individual network nodes, and is believed to be specially suited for cognitive processing (He et al., 2008; Sporns and Zwi, 2004). However, it should be noted that a high value in small-world index, a quantitative measure of small-world topology, could also be observed in highly segregated yet poorly integrated networks due to a lack of long-distance connections (Rubinov and Sporns, 2010). The modular organization implies that the brain networks can be decomposed into subsystems or modules of interconnected brain regions, and is thought to confer robustness and adaptability to the brain networks (Meunier et al., 2010). In previous neuroimaging investigations, the small-world architecture and modular organization have been shown to be disrupted in various brain diseases, such as Alzheimer's disease (He et al., 2008; Pereira et al., 2016; Yao et al., 2010), schizophrenia (Alexander-Bloch et al., 2010; Liu et al., 2008; Zhang et al., 2012) and depression (Chen et al., 2017; Zhang et al., 2011). In ALS, several graph theoretical analyses have been conducted to examine the topological changes of both the resting-state functional networks (Geevasinga et al., 2017; Iyer et al., 2015) and diffusion-based anatomical networks (Buchanan et al., 2015; Dimond et al., 2017; Verstraete et al., 2011; Verstraete et al., 2014). Results obtained by these studies however are inconsistent (even within studies using the same imaging modality): while some studies showed a significant increase in clustering coefficient (Geevasinga et al., 2017; Iyer et al., 2015) and characteristic path length (Dimond et al., 2017), others found no changes at all (Buchanan et al., 2015; Verstraete et al., 2011). Moreover, all of these studies were limited in examining small samples of ALS patients. Of note, to date no study has been performed to examine the modular organization of the brain networks in ALS patients.

In recent years, covariance of brain morphology has been suggested to be a valuable tool to infer large-scale structural brain networks (i.e., structural covariance networks). A key assumption underlying this methodology is that the morphological characteristics of interconnected brain regions would covary since they share common developmental and maturational influences (Alexander-Bloch et al., 2013). It has been shown that structural covariance networks correspond with functional networks and anatomical networks constructed through white matter tractography (Bruno et al., 2017; Hosseini et al., 2016). However, such correspondence should not be considered to be in a connection-by-connection manner, as structural covariance networks in themselves carry unique and meaningful information such as synchronized maturation between brain areas (Alexander-Bloch et al., 2013; Bruno et al., 2017). Furthermore, the construction of structural covariance networks requires relatively lower computational loads (Yao et al., 2010) and is arguably less sensitive to noise in contrast to those of functional and diffusion-based anatomical networks (Bernhardt et al., 2011; Bethlehem et al., 2017). To the best of our knowledge, the structural covariance networks in ALS remain unexplored. More importantly, given that ALS has recently been proposed to be driven by cortical pathologies (Eisen et al., 2017), such as intracellular inclusions of TDP-43 (Braak et al., 2013; Brettschneider et al., 2013), structural covariance network analysis based on gray matter morphology may provide new insights into the pathophysiology of this disease.

In the present study, we used graph theory to examine the topological abnormalities of structural covariance networks for a relatively large sample of ALS patients ($N = 60$) compared with age- and sex-matched normal controls (N = 60). More specifically, a few global network parameters, such as small-world parameters, modularity and global efficiency, as well as two regional network parameters including nodal degree and betweenness centrality, were calculated to characterize the topological organization of the structural covariance networks of the two groups. We hypothesized that the structural covariance networks of ALS patients would show suboptimal topological organization evidenced by altered global network parameters, such as decreased global efficiency, altered small-world parameters and modularity, and also regional network parameters, such as decreased nodal degree and/or betweenness centrality.

2. Materials and methods

2.1. Subjects

One hundred and twenty-eight patients with a diagnosis of sporadic probable or definite ALS according to the revised El Escorial criteria were recruited from 2013 to 2018 (Brooks et al., 2000). Participants underwent clinical examination on the day of MRI examination. All patients were assessed and assigned a score for 'ALS Functional Rating Scale-Revised' (ALSFRS-R) (Cedarbaum et al., 1999). Clinical variables of 'disease duration', measuring the temporal extent from the symptom onset to the scanning date (in months) and 'rate of disease progression', defined as (48-ALSFRS-R)/(disease duration), were also obtained. All patients included in the present study had not received any specific medication. Exclusion criteria were: (1) clinical diagnosis of frontotemporal dementia (Brooks et al., 2000; Rascovsky et al., 2011); (2) family history of motor system diseases; (3) major neurological or psychiatric disorders; and (4) cognitive impairment (Montreal Cognitive Assessment (MoCA) score < 26) (Nasreddine et al., 2005). As displayed in the flow chart for patient inclusion and exclusion (**Fig. S1** in Supplementary Materials), a total of 68 patients were excluded from this study, 5 for major neurological disorders and 63 for MoCA score < 26. At last, 60 patients (39 men and 21 women) were included in the current study. Sixty normal controls (39 men and 21 women) with no history of neurological or psychiatric conditions and with normal brain MRI were recruited from the local community. All participants were right-handed based on measurements of the Edinburgh inventory. Detailed demographic data of all participants are shown in Table 1. The study was conducted in agreement with the Code of Ethics of the World Medical Association (Declaration of Helsinki, 1967). Ethical approval for all procedures was obtained in advance (the Medical Research Ethics Committee of the Southwest Hospital), with written informed consent obtained from all participants.

Table 1
Demographic data of the participants.

	ALS patients (N = 60)	Normal controls (*N* = 60)	*P* value
Mean Age in Years (range)	48.77(26–69)	48.15(24–70)	0.73
Male/female	39/21	39/21	1.00
Education Level in Years (range)	12.2 (5–18)	12.7 (6–19)	0.48
MoCA Score (range)	27.38 (26–30)	27.63 (26–30)	0.29
Limb/bulbar/both onset	47/12/1	–	–
Classic/LMN-D/UMN-D/PLS/PMA	43/7/7/2/1	–	–
Mean Disease Duration in Months (range)	21.05(2 − 132)	–	–
Mean ALSFRS-R (range)	32.62(16–45)	–	–
Mean Disease Progression Rate (range)	1.36(0.02–6.50)	–	–

MoCA = Montreal Cognitive Assessment; The ALS patients were subdivided into 5 phenotypes: classic, lower motor neuron dominant (LMN-D), upper motor neuron dominant (UMN-D), primary lateral sclerosis (PLS) and progressive muscular atrophy (PMA).

2.2. MRI data acquisition and preprocessing

Subjects were imaged with a Siemens 3 T Tim Trio scanner using an eight-channel head coil. High-resolution T1-weighted structural MRI scans were acquired using a magnetization-prepared rapid gradient-echo imaging sequence (repetition time = 1900 ms, echo time = 2.52 ms, inversion time = 900 ms, flip angle = 9°, matrix = 256 × 256, thickness = 1.0 mm, no gap, 176 slices, and voxel size = 1× 1 × 1 mm^3).

Image preprocessing was performed using the Statistical Parametric Mapping 8 (SPM8; Functional Imaging Laboratory, Wellcome Department of Imaging Neuroscience, Institute of Neurology, London, UK; http://www.fil.ion.ucl.ac.uk/spm) VBM8 toolbox (http://www.neuro.uni-jena.de/vbm/download/). All structural images were segmented into gray matter (GM), white matter (WM), and cerebrospinal fluid. The GM images were normalized to the Montreal Neurological Institute space using high-dimensional DARTEL normalization. Images were then modulated to ensure that actual GM volumes were well preserved following spatial normalization.

2.3. Construction of structural covariance networks

As has been done in previous graph theoretical analyses of structural covariance networks, we generated 90 cortical and subcortical regions of interest (ROIs), excluding the cerebellum, from the Automated Anatomical Labeling atlas (Tzourio-Mazoyer et al., 2002). These ROIs were used to mask the individual modulated GM images obtained from voxel-based morphometry and extract the average volume of each ROI. A linear regression analysis was performed at every ROI to remove the effects of age, gender and mean overall GM volume. The residuals of this regression, hereafter referred as corrected GM volumes, were used to construct structural covariance networks (He et al., 2007). Specifically, a correlation matrix $R = [r_{ij}]$ ($i = 1…N$, $j = 1…N$, here $N = 90$) of each group was derived by calculating the Pearson correlation coefficients across individuals between the corrected GM volumes of every pair of regions. The diagonal elements of the correlation matrix were then set to zero to eliminate self-loops. Only positive correlations of the correlation matrix were considered, and negative correlations were assigned a value of zero before further network analysis. From the correlation matrix, a binary adjacency matrix, $A = [a_{ij}]$, was obtained where a_{ij} is 1 if the absolute value of the correlation coefficient r_{ij} between regions i and j is greater than a specific threshold and 0 otherwise. The resultant adjacency matrix A represented a binary undirected graph $G\ (N, E)$, where N is the number of nodes and E is the number of edges. Here, nodes represent brain regions and edges represent undirected links between nodes, which correspond to the nonzero elements in A.

2.4. Global network parameters

Several global network parameters, including clustering coefficient, path length, small-world index, global efficiency, local efficiency, and modularity, were employed to characterize the topological organization of the structural covariance networks (Rubinov and Sporns, 2010). Among these parameters, the clustering coefficient, path length and small-world index are the most widely-used parameters for quantifying the small-world topology of a network. Briefly, the clustering coefficient of a node is defined as the ratio of the number of existing edges to the number of all possible edges in the node's direct neighbors. The clustering coefficient of a network is defined as the average of clustering coefficients over all nodes and reflects network segregation. The shortest path length between two nodes is defined as the minimum number of edges that separates them. The characteristic path length of a network is defined as the average shortest path length between pairs of nodes in a network and reflects network integration. As seen in previous studies (He et al., 2008; He et al., 2007), the fascinating properties of small-world networks were demonstrated through comparisons with random networks that did not show any systemic organization of nodes and edges. The clustering coefficient and characteristic path length of each network were normalized to the corresponding mean values of matched random networks. The small-world index is defined as the ratio of normalized clustering coefficient to normalized path length. The global efficiency is defined as the inverse of the harmonic mean of the shortest path lengths across pairs of nodes in a network. The local efficiency of a node is defined as the global efficiency of the subgraph composed of the nearest neighbors of the node. The local efficiency of a network is defined as the average of local efficiencies across all nodes. The modularity (Blondel et al., 2008) quantifies the degree to which a network can be decomposed into sub-networks (modules) that have maximal intra-module connections and minimal inter-module connections.

2.5. Regional network parameters

Nodal degree and nodal betweenness centrality were used to identify the regional alterations of the structural covariance networks. Nodal degree is defined as the number of connections that a node has with the rest of the network and is considered a measure of the node's interaction within the network. Nodal betweenness centrality is defined as the fraction of all shortest paths in the network that pass through a given node, relative to the total number of shortest paths. Prior to group comparison, the nodal degree and the nodal betweenness centrality were normalized by the average network degree and betweenness centrality, respectively.

2.6. Network hubs

Hubs of a network are nodes that play a critical role in the control of information flow over the network. In this study, a node was considered as a hub if its nodal betweenness centrality is at least one standard deviation higher than the average network betweenness centrality (Bassett et al., 2008; Hosseini et al., 2013).

2.7. Statistical analyses

Graph analysis toolbox (Hosseini et al., 2012) was used to compare the structural covariance networks between ALS patients and controls. Thresholding the correlation matrices with an absolute value results in different numbers of nodes and edges, which may introduce a confound for subsequent between-group comparisons. To solve this problem, the correlation matrix of each group can be thresholded into a binary

adjacency matrix with a network density D, which is defined as the number of edges in a graph divided by the maximum possible number of edges. In this study, a wide range of network densities of $0.10 \leq D \leq 0.42$ were used. The lower limit of the range was the minimum density where the networks of both groups were not fragmented (Here $D_{min} = 0.10$). The upper limit of the range was the maximum density (Here $D_{max} = 0.42$) where the networks of both groups had small-world indices > 1.2 (Hosseini et al., 2013).

Nonparametric permutation testing (1000 repetitions) was conducted to test the statistical significance of the ALS-related differences in global and regional network parameters (Bruno et al., 2017; He et al., 2008). In each permutation, the corrected GM volumes of each participant were randomly reassigned to one of the two new groups with the same number of participants as the original groups. Correlation matrices in each randomized group were constructed and thresholded across the range of network densities. The network parameters were computed for each network at each density. Between-group differences in the network parameters for the two randomized groups were then computed to create a permutation distribution of difference under the null hypothesis. For each network parameter, the actual difference between ALS patients and controls was placed in its corresponding permutation distribution to obtain the significance level. Furthermore, the area under the curve (AUC) was calculated as a summary metric to evaluate the overall group-level differences across all densities (Bruno et al., 2017). The significance level was set at $P < .05$ for group differences in global network parameters. The significance level for group differences in regional network parameters was set at $P < .05$ after false discovery rate correction for multiple comparisons.

3. Results

3.1. Global network analysis

The correlation matrices of the two groups showed that strong correlations exist between most homotopic brain regions (Fig. 1). The global network parameters for each group at a range of densities (0.10–0.42) are displayed in Fig. 2. We found that the structural covariance networks of both groups had a small-world topology across the range of densities, namely, normalized path length close to 1 (Fig. 2A) and normalized clustering higher than 1 (Fig. 2B), or small-world index > 1.2 (Fig. 2C). Compared with normal controls, ALS patients showed significant increases in normalized path length, normalized clustering coefficient, small-world index and local efficiency, and significant decreases in global efficiency at several network densities (Fig. 3). Summary AUC analyses of these indices revealed significantly increased normalized clustering coefficient ($P = .02$), normalized path length ($P = .03$) and small-world index ($P = .03$), as well as significantly decreased global efficiency ($P = .04$) in ALS patients compared with normal controls.

For several network densities, the structural covariance networks of the ALS patients had higher modularity than those of normal controls (Fig. 3F). Subsequent AUC analysis revealed significant modularity increase ($P = .03$) in ALS patients compared with normal controls. Specifically, we identified four modules in normal controls which were designated as the “Frontal-Operculum” module, the “Parietal-Occipital” module, the “Central” module and the “Temporal-Subcortical” module (Fig. 4A). In ALS patients we identified six modules which were designated as the “Frontal” module, the “Operculum” module, the “Occipital” module, the “Parietal-Temporal” module, the “Central” module and the “Temporal-Subcortical” module (Fig. 4B). In short, the “Frontal-Operculum” module and the “Parietal-Occipital” module of normal controls were segregated into two smaller and more local modules in ALS patients-the “Frontal” module and the “Operculum” module, and the “Occipital” module and the “Parietal-Temporal” module, respectively. Although the “Central” and the “Temporal-Subcortical” module were identified in both groups, some differences existed in the size and composition for these modules. For the detailed composition of each module, see **Table S2** in Supplementary materials.

3.2. Regional network analysis

Compared with normal controls, we found decreased nodal degree in the right gyrus rectus (GR) and Heschl's gyrus (HG) in ALS patients (Fig. 5A). Compared with normal controls, both decreased and increased betweenness centrality were found in ALS patients (Fig. 5B). The ALS-related decrease in nodal betweenness was found in the right GR; the ALS-related increase in betweenness centrality was found in the left posterior cingulate cortex (PCC), left triangular part of inferior frontal gyrus (IFG), right supplementary motor area (SMA) and right supramarginal gyrus (SMG).

3.3. Network hub analysis

Compared with normal controls, a different number and distribution of network hubs were found in ALS patients. Specifically, we identified seven network hubs (Fig. 6A) in normal controls (seven cortical) and 11 network hubs (Fig. 6B) in ALS patients (three subcortical, eight cortical). The hub locations were distributed in frontal, temporal, parietal, and occipital cortical regions as well as subcortical regions. The bilateral medial orbitofrontal cortex was common in both groups.

4. Discussion

Here we investigated the topological organization of the structural covariance networks of ALS patients. Compared with normal controls, we found that structural covariance networks of ALS patients showed a consistent rearrangement towards a regularized architecture, as indicated by increased normalized path length, normalized clustering coefficient, small-world index, and modularity, as well as decreased global efficiency, suggesting inefficient global integration and increased local segregation. In addition to the alterations in global network parameters, regional network parameters were affected, showing both decreased and increased nodal betweenness/degree in ALS patients compared with normal controls. We also found a different number and distribution of network hubs in ALS patients compared with normal controls. These findings provide insights into our understanding of the altered topological organization in the structural covariance networks of ALS.

4.1. ALS-related alterations in global network parameters

The structural covariance networks of both ALS patients and controls showed a small-world topology evidenced by higher clustering and comparable path length relative to random networks. Brain networks organized as such permit both specialized (segregated) and integrated information processing, thereby maximizing the efficiency of information propagation while minimizing wiring costs (Achard and Bullmore, 2007; Kaiser and Hilgetag, 2006). Our results provide further evidence for the notion that small-world topology is a fundamental organizational principle of structural brain networks.

Despite the presence of a small-world topology, there were significant group differences in several global network parameters. ALS patients showed significantly increased normalized path length and normalized clustering coefficient in their structural covariance networks compared with normal controls. Likewise, network efficiency analysis revealed significantly decreased global efficiency in ALS patients compared with normal controls. On the one hand, the increase in normalized path length and the decrease in global efficiency, which are in agreement with some previous diffusion MRI network studies (Dimond et al., 2017), reflect disrupted global integration of the structural covariance networks and may be attributable to decreased long-range connections in ALS patients (He et al., 2009; Latora and

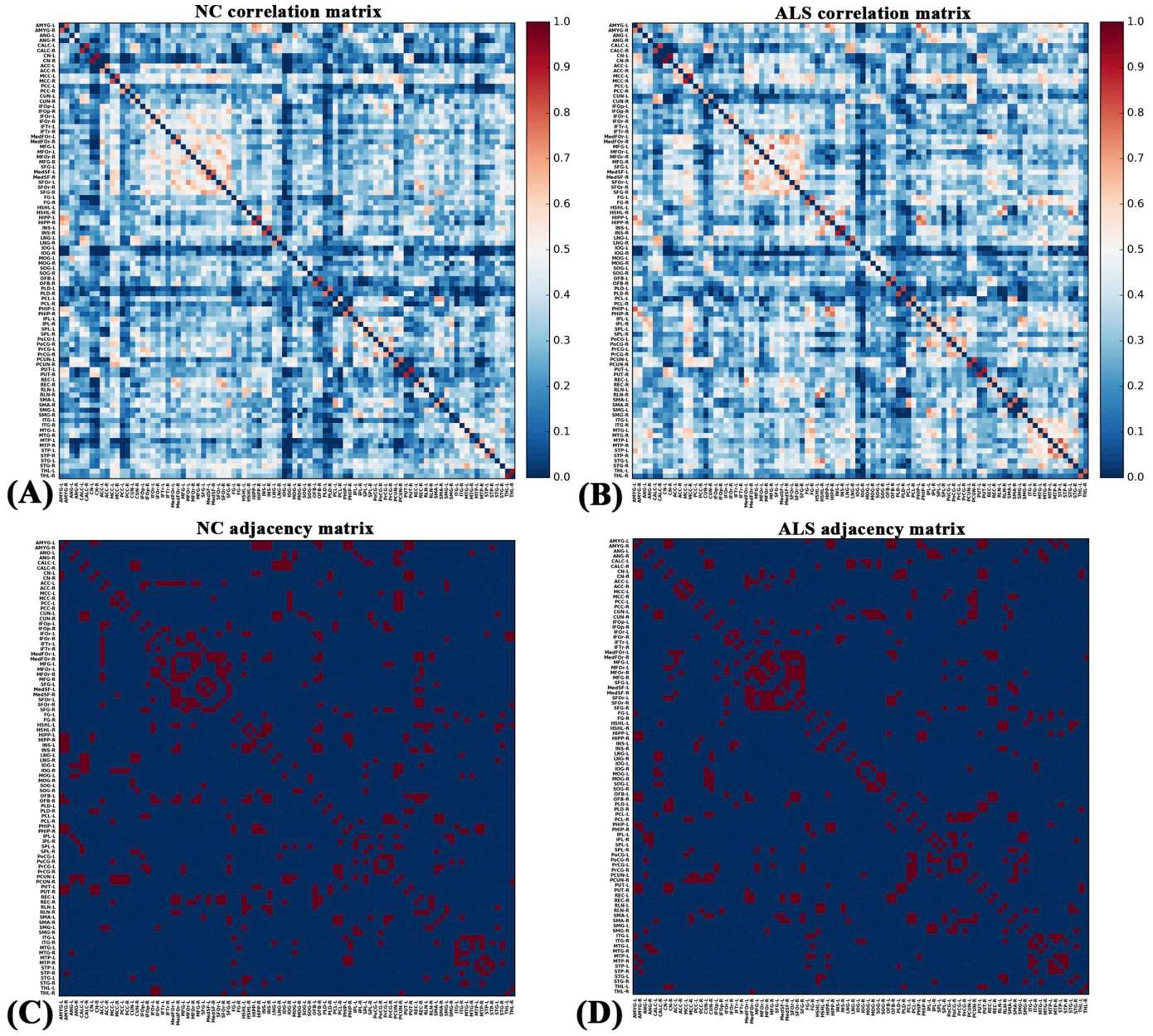

Fig. 1. Correlation and binary adjacency matrices for normal controls (NC) and ALS patients. Correlation matrices for (A) NC and (B) ALS patients, and binary adjacency matrices thresholded at $D_{\min}$ for (C) NC and (D) ALS patients. The color bar denotes the correlation coefficient and represents the strength of the connections.

Marchiori, 2001). On the other hand, the increase in normalized clustering coefficient suggest a stronger local segregation of the structural covariance networks and may be associated with increased short-range connections in ALS patients (He et al., 2009; Latora and Marchiori, 2001). Compared with normal controls, we found an increased small-world index (the ratio of normalized clustering coefficient to normalized path length) in ALS patients, suggesting that alteration in the small-world topology of ALS patients is predominantly driven by the increase in local clustering rather than by the increase in path length. Here, the increase in small-world index should not be thought of as a sign of enhanced small-world architecture, but rather should be considered as an indicator of a more segregated yet less integrated network organization (Rubinov and Sporns, 2010; Strogatz, 2001), in keeping with the results obtained for the individual small-world parameters mentioned above.

More interestingly, our analysis showed a significant modularity increase in ALS patients, suggesting that the structural covariance networks of ALS patients are fragmented into more tightly-clustered modules with poorer inter-module communications. In our study, we identified four modules in normal controls, i.e., the “Frontal-Operculum” module, the “Parietal-Occipital” module, the “Central” module and the “Temporal-Subcortical” module. This finding is consistent with some previous network studies. For example, the ‘Central’ module identified in this study roughly corresponds to the ‘Central’ module obtained in resting-state fMRI networks (Meunier et al., 2009) and the sensorimotor module obtained in structural covariance networks using cortical thickness correlations (Chen et al., 2008). In contrast to normal controls, two more modules (namely six modules) were identified in ALS patients. Notably, the “Frontal-Operculum” module and the “Parietal-Occipital” module of normal controls segregated into two smaller and more local modules in ALS patients, namely, the “Frontal” module and the “Operculum” module, and the “Occipital”

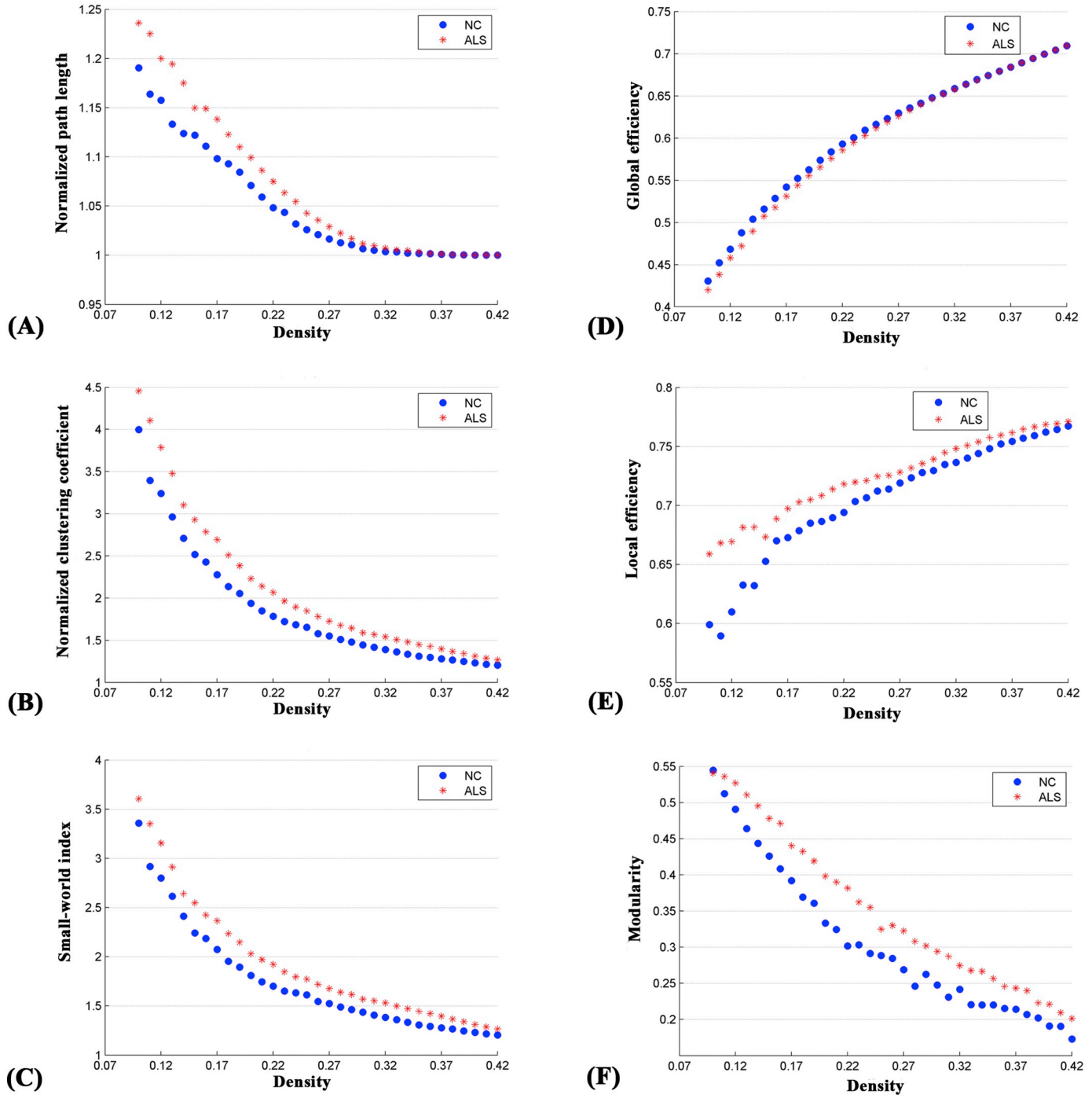

Fig. 2. Changes in global network parameters as a function of network density. (A) normalized path length, (B) normalized clustering coefficient, (C) small-world index, (D) global efficiency, (E) local efficiency and (F) modularity in normal controls (NC) and ALS patients.

module and the "Parietal-Temporal" module, respectively. This finding may be the result of more intra-modular connections (short-range connections or unimodal connections) and less inter-modular connections (long-range connections or cross-modal connections) (Meunier et al., 2010; Westphal et al., 2017), which is also compatible with the aforementioned increases in the normalized clustering coefficient and the normalized path length. In previous network analyses, increases in modularity have been reported in several brain diseases such as Parkinson's disease (Baggio et al., 2014), mild cognitive impairment and Alzheimer's disease (Pereira et al., 2016), which were associated with worse memory and visuospatial performance (Baggio et al., 2014; Westphal et al., 2017). This suggests that they represent pathological alterations and are related to greater clinical decline. Hence, the modularity increase could reflect the imbalance between global integration and local segregation that may underlie the motor and cognitive deficits in ALS patients.

Taken together, alterations in these global network parameters indicate a consistent rearrangement towards a regularized architecture, namely a network configuration that was shown to be associated with reduced signal propagation speed and synchronizability relative to small-world networks (Strogatz, 2001), and therefore a suboptimal topological organization of the structural covariance networks of ALS patients.

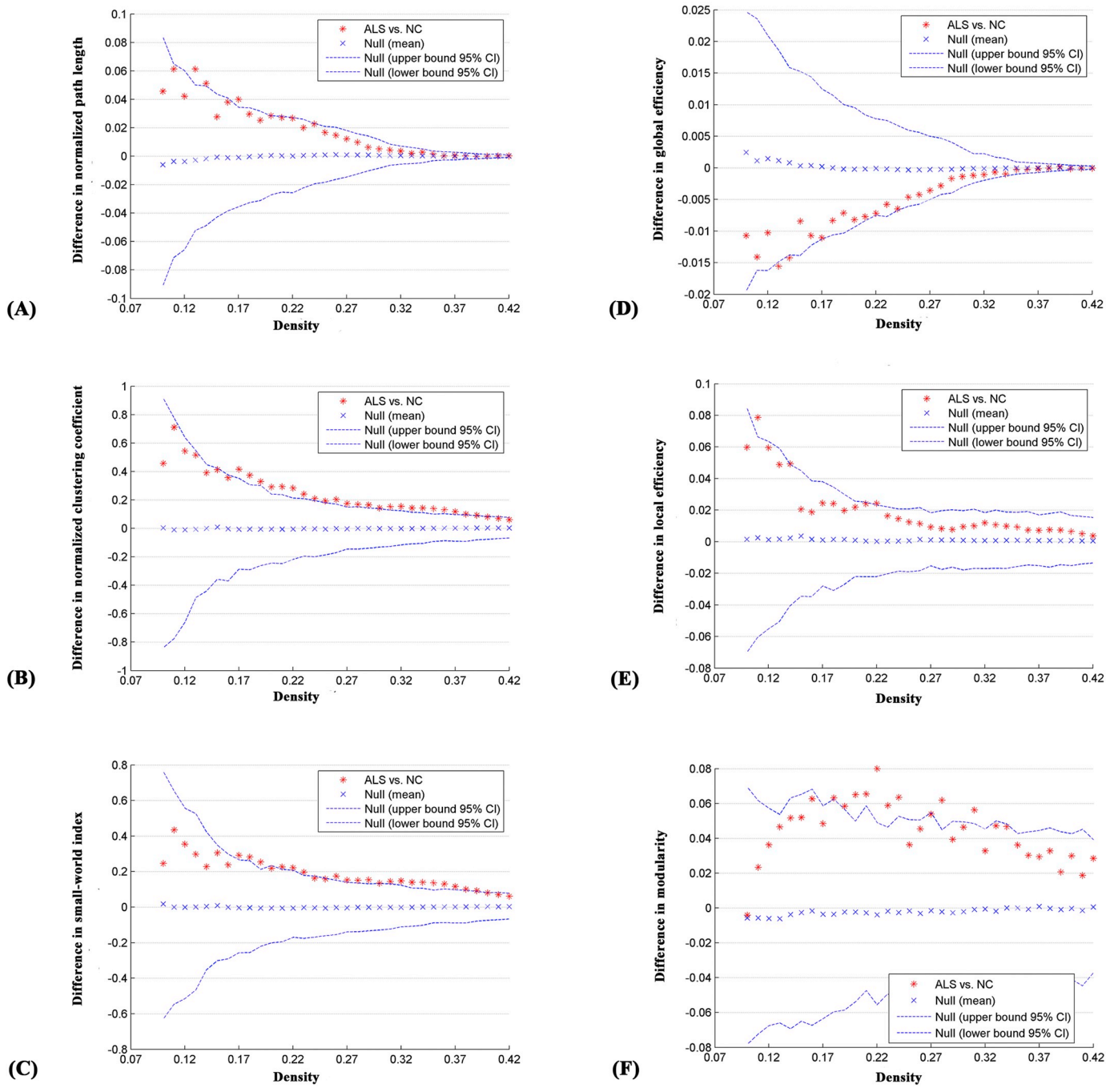

Fig. 3. Differences between normal controls (NC) and ALS patients in global network parameters as a function of network density. The 95% confidence interval and group differences in (A) normalized path length, (B) normalized clustering coefficient, (C) small-world index, (D) global efficiency, (E) local efficiency and (F) modularity. The * marker denotes the difference between NC and ALS patients; the * signs lying outside of the confidence intervals indicate the density where the difference is significant at $P < .05$. The positive values indicate ALS patients > NC and negative values indicate ALS patients < NC.

4.2. ALS-related alterations in regional network parameters

Compared with normal controls, we found a significantly decreased nodal degree in the GR and HG of ALS patients. We also showed decreased nodal betweenness in the GR of ALS patients compared with normal controls. The GR is the medial part of the orbitofrontal cortex, and abnormalities in this region have been associated with deficits in social cognition including facial emotion recognition, empathy and theory of mind (ToM; i.e., the ability to infer mental states of oneself and others) (Bechara, 2004; Schneider and Koenigs, 2017). Converging evidence has demonstrated that recognition of facial expressions of anger, sadness, disgust and surprise, as well as some aspects of ToM are differentially impaired in ALS patients (Bora, 2017; Meier et al., 2010; Sedda, 2014; van der Hulst et al., 2015). Dysfunctions in emotion recognition in ALS patients have been related to the alteration of white-matter integrity along the right inferior longitudinal fasciculus and inferior fronto-occipital fasciculus, which link the occipital cortices to temporo-limbic and orbitofrontal regions, respectively (Crespi et al., 2014). Our finding of decreased nodal degree and betweenness in GR is supported by the histopathological stages of TDP-43 proteinopathy in postmortem ALS brains showing TDP-43 inclusions in the GR at stage 3 (Braak et al., 2013; Brettschneider et al., 2013). The HG, predominately

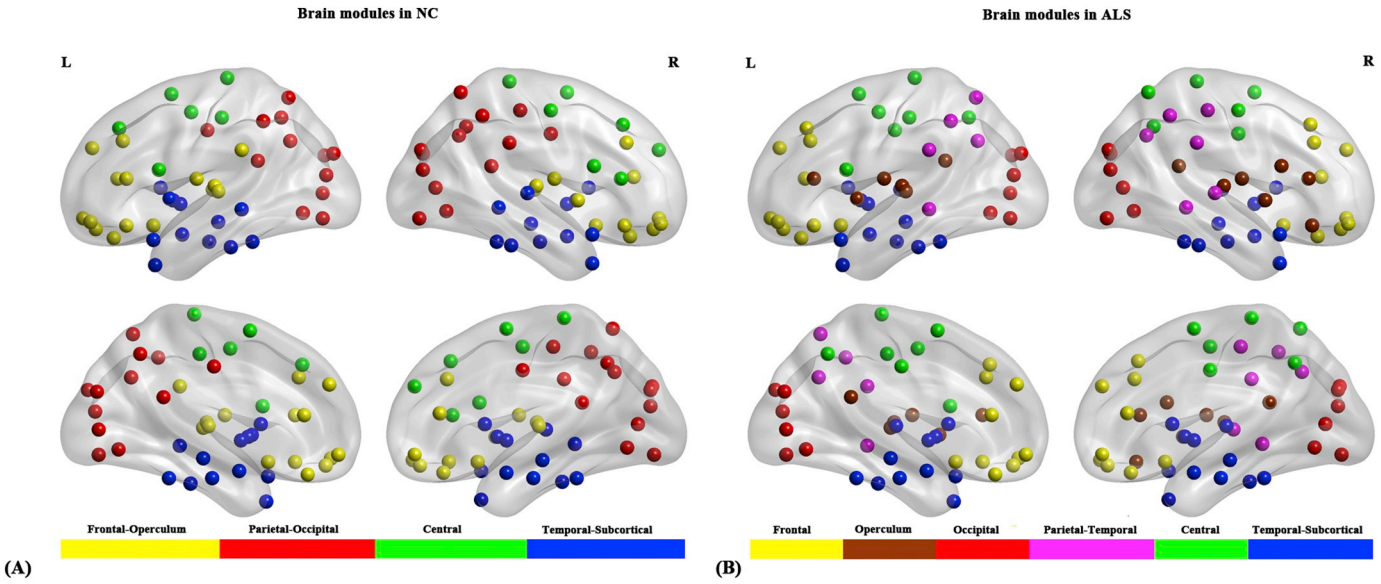

Fig. 4. Brain modules in normal controls (NC) and ALS patients. (A) Four modules were identified in NC and (B) six modules were identified in ALS patients.

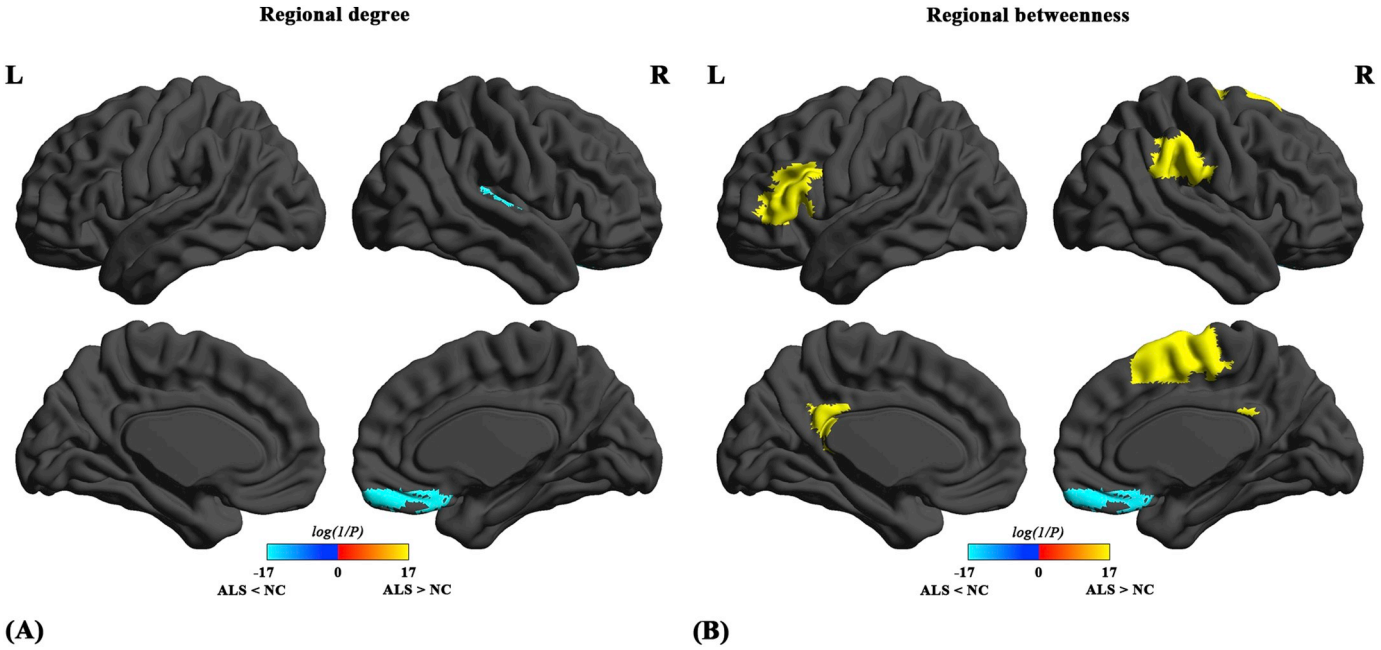

Fig. 5. Differences between normal controls (NC) and ALS patients in regional network parameters. Regions that showed significant differences between ALS patients and NC in regional degree (A) and regional betweenness (B) for networks thresholded at minimum density. The color bar indicates *log(1/P)*. Warm colors denote regions with significantly higher nodal degree or betweenness in ALS patients than in NC, while cool colors denote regions with significantly higher nodal degree or betweenness in NC than in ALS patients.

encompassing the primary auditory cortex, plays a central role in pitch perception (Hall and Plack, 2009; Tang et al., 2017) and is crucial for speech perception and comprehension (Ahissar et al., 2001; de Heer et al., 2017; Friederici, 2011). Our finding of decreased nodal degree in the HG is in agreement with several previous studies, which showed decreased degree centrality (Zhou et al., 2016), *N*-acetylaspartate/choline (Verma et al., 2013) and white matter fractional anisotropy (Lule et al., 2010) in the HG of ALS patients. Notably in the 3rd stage of TDP-43 proteinopathy, intracellular inclusions of TDP-43 have also been documented in the middle and superior temporal gyrus (Braak et al., 2013; Brettschneider et al., 2013). However, the exact functional correlate of the decreased nodal degree in the HG remains unclear. Presumably, a decrease in the nodal degree in the HG may relate to impairments in prosodic recognition (Zimmerman et al., 2007) as well as in the recognition of both sarcastic and paradoxical sarcastic statements (Staios et al., 2013) in ALS patients. These findings, together with a previous diffusion-based network report of decreased nodal degree in the GR and HG of patients with the behavioral variant of FTD (Agosta et al., 2013b), provide new evidence for a continuum between ALS and FTD.

The present study also showed significantly increased nodal betweenness in several brain regions in ALS patients, including the SMA, the triangular part of IFG, the PCC and the SMG. The increased nodal betweenness in these regions in ALS patients implies that the number of shortest paths passing through these regions is higher than those of the control group, suggesting that the information transfer through these regions is more efficient in ALS patients. Our findings are in agreement with previous task-based fMRI studies, which demonstrated increased

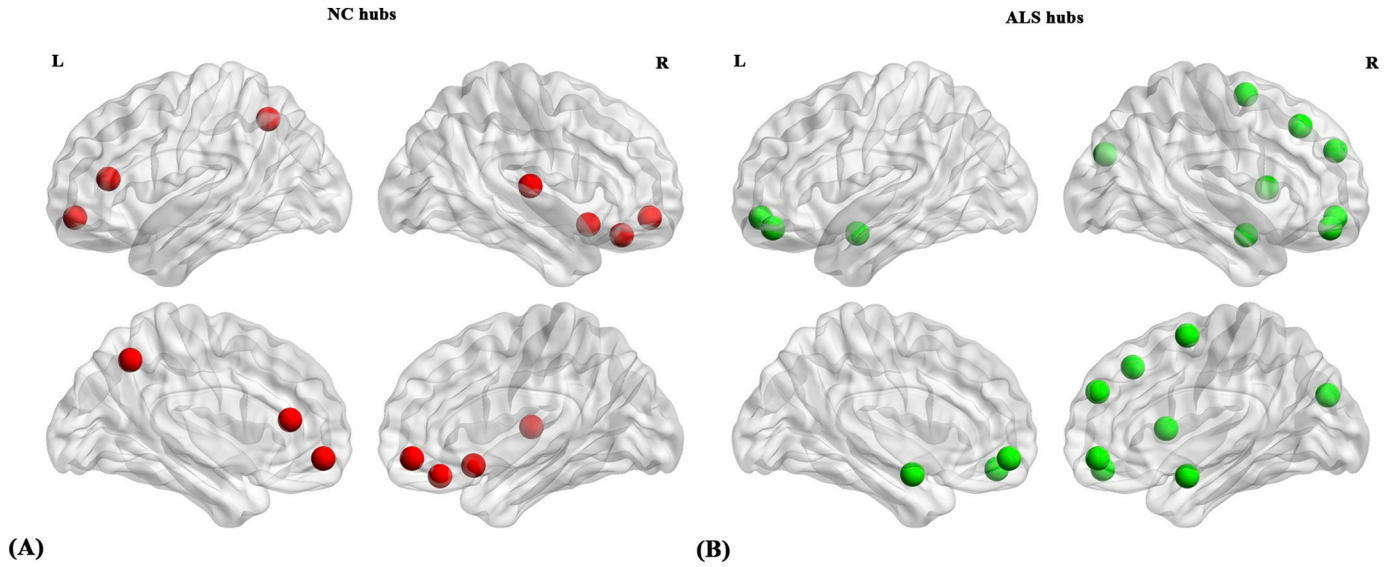

Fig. 6. Network hubs in normal controls (NC) and ALS patients. (A) Seven network hubs (cortical) were identified in NC and (B) 11 network hubs (cortical and subcortical) were identified in ALS patients.

activations in several brain regions of ALS patients including the SMA (Cosottini et al., 2012; Konrad et al., 2002; Konrad et al., 2006; Li et al., 2015), IFG (Palmieri et al., 2010), and SMG (Cosottini et al., 2012; Lule et al., 2007). In addition, resting-state fMRI studies reported increased amplitude of low frequency fluctuation in the IFG (Luo et al., 2012) and increased functional connectivity of the PCC (Heimrath et al., 2014; Menke et al., 2016), SMG (Agosta et al., 2013a; Douaud et al., 2011; Geevasinga et al., 2017; Heimrath et al., 2014) and IFG (Geevasinga et al., 2017; Loewe et al., 2017) in ALS patients.

The SMA is directly connected to the motor cortex and has been shown to play important roles in motor planning and executions (Cona and Semenza, 2017; Vergani et al., 2014). The triangular part of the left IFG is a portion of Broca's area, which is critical for speech production (Fazio et al., 2009; Flinker et al., 2015; Friederici, 2011) and has been implicated in various aspects of language processing (Amunts et al., 2004; Fazio et al., 2009; Nishitani et al., 2005). The SMG, a heteromodal association area, is known to be crucial for both social cognition and language processing (such as semantic processing) (Bzdok et al., 2016; Hartwigsen et al., 2010; Silani et al., 2013). The PCC is a key node of the default mode network, which plays a central role in supporting internally directed cognition (Leech and Sharp, 2014), such as memory retrieval, thinking about future, and inferring the perspectives and thoughts of other people (i.e., ToM) (Buckner et al., 2008). The increased nodal betweenness in these regions may represent neuroplastic reorganizations to compensate (albeit in a futile way) for the motor, language, behavioral and cognitive deficits in ALS patients. In addition to the above-mentioned compensatory mechanism, the hypothesis of cortical hyperexcitability mediated via glutamate excitotoxicity (Kiernan et al., 2011; Turner and Kiernan, 2012) could also be used to explain the increased nodal betweenness in these regions. Of note, PET studies using the benzodiazepine GABAA receptor ligand [C^{11}]fumazenil have shown decreased fumazenil binding in widespread brain regions, including the motor cortex, SMA and Broca's area, in ALS patients, suggesting a loss of inhibitory interneuronal GABA-ergic influence (Lloyd et al., 2000; Turner et al., 2005). Moreover, several studies have documented an imbalance between excitatory and inhibitory neurotransmitters (such as reduced GABA and increased glutamate-glutamine) in the motor cortex as well as in neighboring subcortical white matter in ALS patients (Foerster et al., 2012; Foerster et al., 2014; Foerster et al., 2013; Han and Ma, 2010). Using spectral dynamic causal modeling, our previous study reported a loss of bidirectional connections between the motor cortex and SMA in ALS patients (Fang et al., 2016), which may indicate a breakdown of the inhibitory circuit, leading to a hyperactive SMA. At the same time, increased functional connectivity of the PCC to multiple brain regions including the precentral gyrus has been associated with higher disease progression in ALS patients (Chenji et al., 2016). The exact physiologic basis of increased nodal betweenness however remains unknown. Future studies with data from more imaging modalities, such as transcranial magnetic stimulation and magnetic resonance spectroscopy, are warranted to further explore this issue.

4.3. Network hub analysis

The ALS patients and normal controls also differed in the number and distribution of network hubs. The seven network hubs found in the normal controls were primarily in frontal and temporal areas, whereas the 11 hubs identified in ALS patients were primarily in frontal and subcortical areas. Similar to the regional network finding described above, the hubs of the HG and GR in normal controls were not retained in ALS patients, which may underlie the deficits in speech processing and social cognition, and may be attributable to neuropathological alterations in these regions (Braak et al., 2013; Brettschneider et al., 2013). Compared with normal controls, more frontal (especially in the orbitofrontal cortex and the superior frontal gyrus) and subcortical regions were identified as hubs in ALS patients. This finding is consistent with previous studies, which reported increased functional connectivity strength in the orbitofrontal cortex and superior frontal gyrus(Ma et al., 2015), increased fractional amplitude of low-frequency fluctuations in the left superior frontal gyrus and right caudate (Ma et al., 2016), increased glucose metabolism in the bilateral amygdala (Cistaro et al., 2012), and increased left amygdala-prefrontal functional connectivity (Passamonti et al., 2013) in ALS patients compared with normal controls. The exact neural mechanisms underlying the finding of more hubs in the frontal and subcortical areas however remain unknown, and again may reflect compensatory recruitment or may be driven by a loss of inhibitory neuronal circuits (Kiernan et al., 2011; Turner and Kiernan, 2012), as has been previously mentioned.

4.4. Limitations

There are some limitations that should be addressed in this study. First, the present study was conducted with a cross-sectional design, which does not allow us to delineate the dynamic development of the

abnormalities in the structural covariance networks in ALS. A longitudinal study may help to elucidate the dynamic changing pattern of the abnormalities as the disease progresses. Second, in the present study, given that there are no individual networks but only a network per group when performing structural covariance network analysis, we could not examine the relationship between network parameters and clinical measures. Third, the absence of a comprehensive evaluation of non-motor symptoms weakened the interpretation of our findings.

4.5. Conclusions

In conclusion, the present study revealed abnormal topological organization of the structural covariance networks in ALS patients. Our findings provide network-level evidence for the concept that ALS is a multisystem disorder with a cerebral involvement extending beyond the motor areas.

Declaration of interest

None.

Funding

This study is supported in part by the National Natural Science Foundation of China (Grant Number 11601184) and the Fundamental Research Funds for the Central Universities (Grant Number 2672018ZYGX2018J075).

Appendix A. Supplementary data

Supplementary data to this article can be found online at https://doi.org/10.1016/j.nicl.2018.101619.

References

Achard, S., Bullmore, E., 2007. Efficiency and cost of economical brain functional networks. PLoS Comput. Biol. 3, e17.
Achard, S., Salvador, R., Whitcher, B., Suckling, J., Bullmore, E., 2006. A resilient, low-frequency, small-world human brain functional network with highly connected association cortical hubs. J. Neurosci. 26, 63–72.
Agosta, F., Valsasina, P., Absinta, M., Riva, N., Sala, S., Prelle, A., Copetti, M., Comola, M., Comi, G., Filippi, M., 2011. Sensorimotor functional connectivity changes in amyotrophic lateral sclerosis. Cereb. Cortex 21, 2291–2298.
Agosta, F., Canu, E., Valsasina, P., Riva, N., Prelle, A., Comi, G., Filippi, M., 2013a. Divergent brain network connectivity in amyotrophic lateral sclerosis. Neurobiol. Aging 34, 419–427.
Agosta, F., Sala, S., Valsasina, P., Meani, A., Canu, E., Magnani, G., Cappa, S.F., Scola, E., Quatto, P., Horsfield, M.A., Falini, A., Comi, G., Filippi, M., 2013b. Brain network connectivity assessed using graph theory in frontotemporal dementia. Neurology 81, 134–143.
Ahissar, E., Nagarajan, S., Ahissar, M., Protopapas, A., Mahncke, H., Merzenich, M.M., 2001. Speech comprehension is correlated with temporal response patterns recorded from auditory cortex. Proc. Natl. Acad. Sci. U. S. A. 98, 13367–13372.
Alexander-Bloch, A.F., Gogtay, N., Meunier, D., Birn, R., Clasen, L., Lalonde, F., Lenroot, R., Giedd, J., Bullmore, E.T., 2010. Disrupted modularity and local connectivity of brain functional networks in childhood-onset schizophrenia. Front. Syst. Neurosci. 4, 147.
Alexander-Bloch, A., Raznahan, A., Bullmore, E., Giedd, J., 2013. The convergence of maturational change and structural covariance in human cortical networks. J. Neurosci. 33, 2889–2899.
Amunts, K., Weiss, P.H., Mohlberg, H., Pieperhoff, P., Eickhoff, S., Gurd, J.M., Marshall, J.C., Shah, N.J., Fink, G.R., Zilles, K., 2004. Analysis of neural mechanisms underlying verbal fluency in cytoarchitectonically defined stereotaxic space–the roles of Brodmann areas 44 and 45. NeuroImage 22, 42–56.
Ash, S., Olm, C., McMillan, C.T., Boller, A., Irwin, D.J., McCluskey, L., Elman, L., Grossman, M., 2015. Deficits in sentence expression in amyotrophic lateral sclerosis. Amyotroph Lateral Scler Frontotemporal Degener 16, 31–39.
Baggio, H.C., Sala-Llonch, R., Segura, B., Marti, M.J., Valldeoriola, F., Compta, Y., Tolosa, E., Junque, C., 2014. Functional brain networks and cognitive deficits in Parkinson's disease. Hum. Brain Mapp. 35, 4620–4634.
Bassett, D.S., Bullmore, E., Verchinski, B.A., Mattay, V.S., Weinberger, D.R., Meyer-Lindenberg, A., 2008. Hierarchical organization of human cortical networks in health and schizophrenia. J. Neurosci. 28, 9239–9248.
Bechara, A., 2004. The role of emotion in decision-making: evidence from neurological patients with orbitofrontal damage. Brain Cogn. 55, 30–40.
Bede, P., Bokde, A., Elamin, M., Byrne, S., McLaughlin, R.L., Jordan, N., Hampel, H., Gallagher, L., Lynch, C., Fagan, A.J., Pender, N., Hardiman, O., 2013. Grey matter correlates of clinical variables in amyotrophic lateral sclerosis (ALS): a neuroimaging study of ALS motor phenotype heterogeneity and cortical focality. J. Neurol. Neurosurg. Psychiatry 84, 766–773.
Bernhardt, B.C., Chen, Z., He, Y., Evans, A.C., Bernasconi, N., 2011. Graph-theoretical analysis reveals disrupted small-world organization of cortical thickness correlation networks in temporal lobe epilepsy. Cereb. Cortex 21, 2147–2157.
Bethlehem, R.A.I., Romero-Garcia, R., Mak, E., Bullmore, E.T., Baron-Cohen, S., 2017. Structural covariance networks in children with autism or ADHD. Cereb. Cortex 27, 4267–4276.
Blondel, V.D., Guillaume, J.-L., Lambiotte, R., Lefebvre, E., 2008. Fast unfolding of communities in large networks. Journal of Statistical Mechanics 2008, P10008.
Bora, E., 2017. Meta-analysis of social cognition in amyotrophic lateral sclerosis. Cortex 88, 1–7.
Braak, H., Brettschneider, J., Ludolph, A.C., Lee, V.M., Trojanowski, J.Q., Del Tredici, K., 2013. Amyotrophic lateral sclerosis–a model of corticofugal axonal spread. Nat. Rev. Neurol. 9, 708–714.
Brettschneider, J., Del Tredici, K., Toledo, J.B., Robinson, J.L., Irwin, D.J., Grossman, M., Suh, E., Van Deerlin, V.M., Wood, E.M., Baek, Y., Kwong, L., Lee, E.B., Elman, L., McCluskey, L., Fang, L., Feldengut, S., Ludolph, A.C., Lee, V.M., Braak, H., Trojanowski, J.Q., 2013. Stages of pTDP-43 pathology in amyotrophic lateral sclerosis. Ann. Neurol. 74, 20–38.
Brooks, B.R., Miller, R.G., Swash, M., Munsat, T.L., World Federation of Neurology Research Group on Motor Neuron, D, 2000. El Escorial revisited: revised criteria for the diagnosis of amyotrophic lateral sclerosis. Amyotroph Lateral Scler Other Motor Neuron Disord 1, 293–299.
Bruno, J.L., Hosseini, S.M.H., Saggar, M., Quintin, E.M., Raman, M.M., Reiss, A.L., 2017. Altered brain network segregation in fragile X syndrome revealed by structural connectomics. Cereb. Cortex 27, 2249–2259.
Buchanan, C.R., Pettit, L.D., Storkey, A.J., Abrahams, S., Bastin, M.E., 2015. Reduced structural connectivity within a prefrontal-motor-subcortical network in amyotrophic lateral sclerosis. J. Magn. Reson. Imaging 41, 1342–1352.
Buckner, R.L., Andrews-Hanna, J.R., Schacter, D.L., 2008. The brain's default network: anatomy, function, and relevance to disease. Ann. N. Y. Acad. Sci. 1124, 1–38.
Bzdok, D., Hartwigsen, G., Reid, A., Laird, A.R., Fox, P.T., Eickhoff, S.B., 2016. Left inferior parietal lobe engagement in social cognition and language. Neurosci. Biobehav. Rev. 68, 319–334.
Cedarbaum, J.M., Stambler, N., Malta, E., Fuller, C., Hilt, D., Thurmond, B., Nakanishi, A., 1999. The ALSFRS-R: a revised ALS functional rating scale that incorporates assessments of respiratory function BDNF ALS Study Group (Phase III). J Neurol Sci 169, 13–21.
Chang, J.L., Lomen-Hoerth, C., Murphy, J., Henry, R.G., Kramer, J.H., Miller, B.L., Gorno-Tempini, M.L., 2005. A voxel-based morphometry study of patterns of brain atrophy in ALS and ALS/FTLD. Neurology 65, 75–80.
Chen, Z.J., He, Y., Rosa-Neto, P., Germann, J., Evans, A.C., 2008. Revealing modular architecture of human brain structural networks by using cortical thickness from MRI. Cereb. Cortex 18, 2374–2381.
Chen, T., Kendrick, K.M., Wang, J., Wu, M., Li, K., Huang, X., Luo, Y., Lui, S., Sweeney, J.A., Gong, Q., 2017. Anomalous single-subject based morphological cortical networks in drug-naive, first-episode major depressive disorder. Hum. Brain Mapp. 38, 2482–2494.
Chenji, S., Jha, S., Lee, D., Brown, M., Seres, P., Mah, D., Kalra, S., 2016. Investigating default mode and sensorimotor network connectivity in amyotrophic lateral sclerosis. PLoS One 11, e0157443.
Cistaro, A., Valentini, M.C., Chio, A., Nobili, F., Calvo, A., Moglia, C., Montuschi, A., Morbelli, S., Salmaso, D., Fania, P., Carrara, G., Pagani, M., 2012. Brain hypermetabolism in amyotrophic lateral sclerosis: a FDG PET study in ALS of spinal and bulbar onset. Eur. J. Nucl. Med. Mol. Imaging 39, 251–259.
Cona, G., Semenza, C., 2017. Supplementary motor area as key structure for domain-general sequence processing: a unified account. Neurosci. Biobehav. Rev. 72, 28–42.
Cosottini, M., Giannelli, M., Siciliano, G., Lazzarotti, G., Michelassi, M.C., Del Corona, A., Bartolozzi, C., Murri, L., 2005. Diffusion-tensor MR imaging of corticospinal tract in amyotrophic lateral sclerosis and progressive muscular atrophy. Radiology 237, 258–264.
Cosottini, M., Pesaresi, I., Piazza, S., Diciotti, S., Cecchi, P., Fabbri, S., Carlesi, C., Mascalchi, M., Siciliano, G., 2012. Structural and functional evaluation of cortical motor areas in amyotrophic lateral sclerosis. Exp. Neurol. 234, 169–180.
Crespi, C., Cerami, C., Dodich, A., Canessa, N., Arpone, M., Iannaccone, S., Corbo, M., Lunetta, C., Scola, E., Falini, A., Cappa, S.F., 2014. Microstructural white matter correlates of emotion recognition impairment in amyotrophic lateral sclerosis. Cortex 53, 1–8.
D'Ambrosio, A., Gallo, A., Trojsi, F., Corbo, D., Esposito, F., Cirillo, M., Monsurro, M.R., Tedeschi, G., 2014. Frontotemporal cortical thinning in amyotrophic lateral sclerosis. AJNR Am. J. Neuroradiol. 35, 304–310.
de Heer, W.A., Huth, A.G., Griffiths, T.L., Gallant, J.L., Theunissen, F.E., 2017. The hierarchical cortical organization of human speech processing. J. Neurosci. 37, 6539–6557.
Dimond, D., Ishaque, A., Chenji, S., Mah, D., Chen, Z., Seres, P., Beaulieu, C., Kalra, S., 2017. White matter structural network abnormalities underlie executive dysfunction in amyotrophic lateral sclerosis. Hum. Brain Mapp. 38, 1249–1268.
Douaud, G., Filippini, N., Knight, S., Talbot, K., Turner, M.R., 2011. Integration of structural and functional magnetic resonance imaging in amyotrophic lateral sclerosis. Brain 134, 3470–3479.
Eisen, A., Braak, H., Del Tredici, K., Lemon, R., Ludolph, A.C., Kiernan, M.C., 2017. Cortical influences drive amyotrophic lateral sclerosis. J. Neurol. Neurosurg.

Psychiatry 88, 917–924.
Fan, Y., Shi, F., Smith, J.K., Lin, W., Gilmore, J.H., Shen, D., 2011. Brain anatomical networks in early human brain development. NeuroImage 54, 1862–1871.
Fang, X., Zhang, Y., Wang, Y., Zhang, Y., Hu, J., Wang, J., Zhang, J., Jiang, T., 2016. Disrupted effective connectivity of the sensorimotor network in amyotrophic lateral sclerosis. J. Neurol. 263, 508–516.
Fazio, P., Cantagallo, A., Craighero, L., D'Ausilio, A., Roy, A.C., Pozzo, T., Calzolari, F., Granieri, E., Fadiga, L., 2009. Encoding of human action in Broca's area. Brain 132, 1980–1988.
Filippini, N., Douaud, G., MacKay, C.E., Knight, S., Talbot, K., Turner, M.R., 2010. Corpus callosum involvement is a consistent feature of amyotrophic lateral sclerosis. Neurology 75, 1645–1652.
Flinker, A., Korzeniewska, A., Shestyuk, A.Y., Franaszczuk, P.J., Dronkers, N.F., Knight, R.T., Crone, N.E., 2015. Redefining the role of Broca's area in speech. Proc. Natl. Acad. Sci. U. S. A. 112, 2871–2875.
Foerster, B.R., Callaghan, B.C., Petrou, M., Edden, R.A., Chenevert, T.L., Feldman, E.L., 2012. Decreased motor cortex gamma-aminobutyric acid in amyotrophic lateral sclerosis. Neurology 78, 1596–1600.
Foerster, B.R., Pomper, M.G., Callaghan, B.C., Petrou, M., Edden, R.A., Mohamed, M.A., Welsh, R.C., Carlos, R.C., Barker, P.B., Feldman, E.L., 2013. An imbalance between excitatory and inhibitory neurotransmitters in amyotrophic lateral sclerosis revealed by use of 3-T proton magnetic resonance spectroscopy. JAMA Neurol 70, 1009–1016.
Foerster, B.R., Carlos, R.C., Dwamena, B.A., Callaghan, B.C., Petrou, M., Edden, R.A., Mohamed, M.A., Welsh, R.C., Barker, P.B., Feldman, E.L., Pomper, M.G., 2014. Multimodal MRI as a diagnostic biomarker for amyotrophic lateral sclerosis. Ann Clin Transl Neurol 1, 107–114.
Friederici, A.D., 2011. The brain basis of language processing: from structure to function. Physiol. Rev. 91, 1357–1392.
Geevasinga, N., Korgaonkar, M.S., Menon, P., Van den Bos, M., Gomes, L., Foster, S., Kiernan, M.C., Vucic, S., 2017. Brain functional connectome abnormalities in amyotrophic lateral sclerosis are associated with disability and cortical hyperexcitability. Eur. J. Neurol. 24, 1507–1517.
Goldstein, L.H., Abrahams, S., 2013. Changes in cognition and behaviour in amyotrophic lateral sclerosis: nature of impairment and implications for assessment. Lancet Neurol. 12, 368–380.
Hall, D.A., Plack, C.J., 2009. Pitch processing sites in the human auditory brain. Cereb. Cortex 19, 576–585.
Han, J., Ma, L., 2010. Study of the features of proton MR spectroscopy ((1)H-MRS) on amyotrophic lateral sclerosis. J. Magn. Reson. Imaging 31, 305–308.
Hartwigsen, G., Baumgaertner, A., Price, C.J., Koehnke, M., Ulmer, S., Siebner, H.R., 2010. Phonological decisions require both the left and right supramarginal gyri. Proc. Natl. Acad. Sci. U. S. A. 107, 16494–16499.
He, Y., Chen, Z.J., Evans, A.C., 2007. Small-world anatomical networks in the human brain revealed by cortical thickness from MRI. Cereb. Cortex 17, 2407–2419.
He, Y., Chen, Z., Evans, A., 2008. Structural insights into aberrant topological patterns of large-scale cortical networks in Alzheimer's disease. J. Neurosci. 28, 4756–4766.
He, Y., Dagher, A., Chen, Z., Charil, A., Zijdenbos, A., Worsley, K., Evans, A., 2009. Impaired small-world efficiency in structural cortical networks in multiple sclerosis associated with white matter lesion load. Brain 132, 3366–3379.
Heimrath, J., Gorges, M., Kassubek, J., Muller, H.P., Birbaumer, N., Ludolph, A.C., Lule, D., 2014. Additional resources and the default mode network: evidence of increased connectivity and decreased white matter integrity in amyotrophic lateral sclerosis. Amyotroph Lateral Scler Frontotemporal Degener 15, 537–545.
Hosseini, S.M., Hoeft, F., Kesler, S.R., 2012. GAT: a graph-theoretical analysis toolbox for analyzing between-group differences in large-scale structural and functional brain networks. PLoS One 7, e40709.
Hosseini, S.M., Black, J.M., Soriano, T., Bugescu, N., Martinez, R., Raman, M.M., Kesler, S.R., Hoeft, F., 2013. Topological properties of large-scale structural brain networks in children with familial risk for reading difficulties. NeuroImage 71, 260–274.
Hosseini, S.M., Mazaika, P., Mauras, N., Buckingham, B., Weinzimer, S.A., Tsalikian, E., White, N.H., Reiss, A.L., Diabetes Research in Children, 2016. Altered integration of structural covariance networks in young children with type 1 diabetes. Hum Brain Mapp 37, 4034–4046.
Iwata, N.K., Kwan, J.Y., Danielian, L.E., Butman, J.A., Tovar-Moll, F., Bayat, E., Floeter, M.K., 2011. White matter alterations differ in primary lateral sclerosis and amyotrophic lateral sclerosis. Brain 134, 2642–2655.
Iyer, P.M., Egan, C., Pinto-Grau, M., Burke, T., Elamin, M., Nasseroleslami, B., Pender, N., Lalor, E.C., Hardiman, O., 2015. Functional connectivity changes in resting-state EEG as potential biomarker for amyotrophic lateral sclerosis. PLoS One 10, e0128682.
Jelsone-Swain, L.M., Fling, B.W., Seidler, R.D., Hovatter, R., Gruis, K., Welsh, R.C., 2010. Reduced interhemispheric functional connectivity in the motor cortex during rest in limb-onset amyotrophic lateral sclerosis. Front. Syst. Neurosci. 4, 158.
Kaiser, M., Hilgetag, C.C., 2006. Nonoptimal component placement, but short processing paths, due to long-distance projections in neural systems. PLoS Comput. Biol. 2, e95.
Kiernan, M.C., Vucic, S., Cheah, B.C., Turner, M.R., Eisen, A., Hardiman, O., Burrell, J.R., Zoing, M.C., 2011. Amyotrophic lateral sclerosis. Lancet 377, 942–955.
Kim, H.J., de Leon, M., Wang, X., Kim, H.Y., Lee, Y.J., Kim, Y.H., Kim, S.H., 2017. Relationship between clinical parameters and brain structure in sporadic amyotrophic lateral sclerosis patients according to onset type: a voxel-based morphometric study. PLoS One 12, e0168424.
Konrad, C., Henningsen, H., Bremer, J., Mock, B., Deppe, M., Buchinger, C., Turski, P., Knecht, S., Brooks, B., 2002. Pattern of cortical reorganization in amyotrophic lateral sclerosis: a functional magnetic resonance imaging study. Exp. Brain Res. 143, 51–56.
Konrad, C., Jansen, A., Henningsen, H., Sommer, J., Turski, P.A., Brooks, B.R., Knecht, S., 2006. Subcortical reorganization in amyotrophic lateral sclerosis. Exp. Brain Res. 172, 361–369.
Latora, V., Marchiori, M., 2001. Efficient behavior of small-world networks. Phys. Rev. Lett. 87, 198701.
Leech, R., Sharp, D.J., 2014. The role of the posterior cingulate cortex in cognition and disease. Brain 137, 12–32.
Li, H., Chen, Y., Li, Y., Yin, B., Tang, W., Yu, X., Huang, W., Geng, D., Zhang, B., 2015. Altered cortical activation during action observation in amyotrophic lateral sclerosis patients: a parametric functional MRI study. Eur. Radiol. 25, 2584–2592.
Liu, Y., Liang, M., Zhou, Y., He, Y., Hao, Y., Song, M., Yu, C., Liu, H., Liu, Z., Jiang, T., 2008. Disrupted small-world networks in schizophrenia. Brain 131, 945–961.
Lloyd, C.M., Richardson, M.P., Brooks, D.J., Al-Chalabi, A., Leigh, P.N., 2000. Extramotor involvement in ALS: PET studies with the GABA(A) ligand [(11)C]flumazenil. Brain 123, 2289–2296 Pt 11.
Loewe, K., Machts, J., Kaufmann, J., Petri, S., Heinze, H.J., Borgelt, C., Harris, J.A., Vielhaber, S., Schoenfeld, M.A., 2017. Widespread temporo-occipital lobe dysfunction in amyotrophic lateral sclerosis. Sci. Rep. 7, 40252.
Lule, D., Diekmann, V., Anders, S., Kassubek, J., Kubler, A., Ludolph, A.C., Birbaumer, N., 2007. Brain responses to emotional stimuli in patients with amyotrophic lateral sclerosis (ALS). J. Neurol. 254, 519–527.
Lule, D., Diekmann, V., Muller, H.P., Kassubek, J., Ludolph, A.C., Birbaumer, N., 2010. Neuroimaging of multimodal sensory stimulation in amyotrophic lateral sclerosis. J. Neurol. Neurosurg. Psychiatry 81, 899–906.
Luo, C., Chen, Q., Huang, R., Chen, X., Chen, K., Huang, X., Tang, H., Gong, Q., Shang, H.F., 2012. Patterns of spontaneous brain activity in amyotrophic lateral sclerosis: a resting-state FMRI study. PLoS One 7, e45470.
Ma, X., Zhang, J., Zhang, Y., Chen, H., Li, R., Wang, J., Chen, H., 2015. Altered cortical hubs in functional brain networks in amyotrophic lateral sclerosis. Neurol. Sci. 36, 2097–2104.
Ma, X., Zhang, J., Zhang, Y., Chen, H., Li, R., Long, Z., Zheng, J., Wang, J., Chen, H., 2016. Frequency-specific alterations in the fractional amplitude of low-frequency fluctuations in amyotrophic lateral sclerosis. Neurol. Sci. 37, 1283–1291.
Meier, S.L., Charleston, A.J., Tippett, L.J., 2010. Cognitive and behavioural deficits associated with the orbitomedial prefrontal cortex in amyotrophic lateral sclerosis. Brain 133, 3444–3457.
Menke, R.A., Korner, S., Filippini, N., Douaud, G., Knight, S., Talbot, K., Turner, M.R., 2014. Widespread grey matter pathology dominates the longitudinal cerebral MRI and clinical landscape of amyotrophic lateral sclerosis. Brain 137, 2546–2555.
Menke, R.A., Proudfoot, M., Wuu, J., Andersen, P.M., Talbot, K., Benatar, M., Turner, M.R., 2016. Increased functional connectivity common to symptomatic amyotrophic lateral sclerosis and those at genetic risk. J. Neurol. Neurosurg. Psychiatry 87, 580–588.
Meunier, D., Achard, S., Morcom, A., Bullmore, E., 2009. Age-related changes in modular organization of human brain functional networks. NeuroImage 44, 715–723.
Meunier, D., Lambiotte, R., Bullmore, E.T., 2010. Modular and hierarchically modular organization of brain networks. Front. Neurosci. 4, 200.
Mohammadi, B., Kollewe, K., Samii, A., Krampfl, K., Dengler, R., Munte, T.F., 2009. Changes of resting state brain networks in amyotrophic lateral sclerosis. Exp. Neurol. 217, 147–153.
Montuschi, A., Iazzolino, B., Calvo, A., Moglia, C., Lopiano, L., Restagno, G., Brunetti, M., Ossola, I., Lo Presti, A., Cammarosano, S., Canosa, A., Chio, A., 2015. Cognitive correlates in amyotrophic lateral sclerosis: a population-based study in Italy. J. Neurol. Neurosurg. Psychiatry 86, 168–173.
Muller, H.P., Turner, M.R., Grosskreutz, J., Abrahams, S., Bede, P., Govind, V., Prudlo, J., Ludolph, A.C., Filippi, M., Kassubek, J., Neuroimaging Society in, A.L.S.D.T.I.S.G, 2016. A large-scale multicentre cerebral diffusion tensor imaging study in amyotrophic lateral sclerosis. J. Neurol. Neurosurg. Psychiatry 87, 570–579.
Murphy, J., Henry, R., Lomen-Hoerth, C., 2007. Establishing subtypes of the continuum of frontal lobe impairment in amyotrophic lateral sclerosis. Arch. Neurol. 64, 330–334.
Nasreddine, Z.S., Phillips, N.A., Bedirian, V., Charbonneau, S., Whitehead, V., Collin, I., Cummings, J.L., Chertkow, H., 2005. The montreal cognitive assessment, MoCA: a brief screening tool for mild cognitive impairment. J. Am. Geriatr. Soc. 53, 695–699.
Neumann, M., Sampathu, D.M., Kwong, L.K., Truax, A.C., Micsenyi, M.C., Chou, T.T., Bruce, J., Schuck, T., Grossman, M., Clark, C.M., McCluskey, L.F., Miller, B.L., Masliah, E., Mackenzie, I.R., Feldman, H., Feiden, W., Kretzschmar, H.A., Trojanowski, J.Q., Lee, V.M., 2006. Ubiquitinated TDP-43 in frontotemporal lobar degeneration and amyotrophic lateral sclerosis. Science 314, 130–133.
Nishitani, N., Schurmann, M., Amunts, K., Hari, R., 2005. Broca's region: from action to language. Physiology (Bethesda) 20, 60–69.
Palmieri, A., Naccarato, M., Abrahams, S., Bonato, M., D'Ascenzo, C., Balestreri, S., Cima, V., Querin, G., Dal Borgo, R., Barachino, L., Volpato, C., Semenza, C., Pegoraro, E., Angelini, C., Soraru, G., 2010. Right hemisphere dysfunction and emotional processing in ALS: an fMRI study. J. Neurol. 257, 1970–1978.
Passamonti, L., Fera, F., Tessitore, A., Russo, A., Cerasa, A., Gioia, C.M., Monsurro, M.R., Migliaccio, R., Tedeschi, G., Quattrone, A., 2013. Dysfunctions within limbic-motor networks in amyotrophic lateral sclerosis. Neurobiol. Aging 34, 2499–2509.
Pereira, J.B., Mijalkov, M., Kakaei, E., Mecocci, P., Vellas, B., Tsolaki, M., Kloszewska, I., Soininen, H., Spenger, C., Lovestone, S., Simmons, A., Wahlund, L.O., Volpe, G., Westman, E., 2016. Disrupted network topology in patients with stable and progressive mild cognitive impairment and Alzheimer's Disease. Cereb. Cortex 26, 3476–3493.
Rascovsky, K., Hodges, J.R., Knopman, D., Mendez, M.F., Kramer, J.H., Neuhaus, J., van Swieten, J.C., Seelaar, H., Dopper, E.G., Onyike, C.U., Hillis, A.E., Josephs, K.A., Boeve, B.F., Kertesz, A., Seeley, W.W., Rankin, K.P., Johnson, J.K., Gorno-Tempini, M.L., Rosen, H., Prioleau-Latham, C.E., Lee, A., Kipps, C.M., Lillo, P., Piguet, O., Rohrer, J.D., Rossor, M.N., Warren, J.D., Fox, N.C., Galasko, D., Salmon, D.P., Black, S.E., Mesulam, M., Weintraub, S., Dickerson, B.C., Diehl-Schmid, J., Pasquier, F., Deramecourt, V., Lebert, F., Pijnenburg, Y., Chow, T.W., Manes, F., Grafman, J.,

Cappa, S.F., Freedman, M., Grossman, M., Miller, B.L., 2011. Sensitivity of revised diagnostic criteria for the behavioural variant of frontotemporal dementia. Brain 134, 2456–2477.
Riku, Y., Watanabe, H., Yoshida, M., Tatsumi, S., Mimuro, M., Iwasaki, Y., Katsuno, M., Iguchi, Y., Masuda, M., Senda, J., Ishigaki, S., Udagawa, T., Sobue, G., 2014. Lower motor neuron involvement in TAR DNA-binding protein of 43 kDa-related frontotemporal lobar degeneration and amyotrophic lateral sclerosis. JAMA Neurol 71, 172–179.
Rubinov, M., Sporns, O., 2010. Complex network measures of brain connectivity: uses and interpretations. NeuroImage 52, 1059–1069.
Schneider, B., Koenigs, M., 2017. Human lesion studies of ventromedial prefrontal cortex. Neuropsychologia 107, 84–93.
Sedda, A., 2014. Disorders of emotional processing in amyotrophic lateral sclerosis. Curr. Opin. Neurol. 27, 659–665.
Senda, J., Ito, M., Watanabe, H., Atsuta, N., Kawai, Y., Katsuno, M., Tanaka, F., Naganawa, S., Fukatsu, H., Sobue, G., 2009. Correlation between pyramidal tract degeneration and widespread white matter involvement in amyotrophic lateral sclerosis: a study with tractography and diffusion-tensor imaging. Amyotroph. Lateral Scler. 10, 288–294.
Senda, J., Atsuta, N., Watanabe, H., Bagarinao, E., Imai, K., Yokoi, D., Riku, Y., Masuda, M., Nakamura, R., Watanabe, H., Ito, M., Katsuno, M., Naganawa, S., Sobue, G., 2017. Structural MRI correlates of amyotrophic lateral sclerosis progression. J. Neurol. Neurosurg. Psychiatry 88, 901–907.
Shen, D., Cui, L., Fang, J., Cui, B., Li, D., Tai, H., 2016. Voxel-wise meta-analysis of gray matter changes in amyotrophic lateral sclerosis. Front. Aging Neurosci. 8, 64.
Silani, G., Lamm, C., Ruff, C.C., Singer, T., 2013. Right supramarginal gyrus is crucial to overcome emotional egocentricity bias in social judgments. J. Neurosci. 33, 15466–15476.
Sporns, O., Zwi, J.D., 2004. The small world of the cerebral cortex. Neuroinformatics 2, 145–162.
Staios, M., Fisher, F., Lindell, A.K., Ong, B., Howe, J., Reardon, K., 2013. Exploring sarcasm detection in amyotrophic lateral sclerosis using ecologically valid measures. Front. Hum. Neurosci. 7, 178.
Strogatz, S.H., 2001. Exploring complex networks. Nature 410, 268–276.
Swinnen, B., Robberecht, W., 2014. The phenotypic variability of amyotrophic lateral sclerosis. Nat. Rev. Neurol. 10, 661–670.
Tang, C., Hamilton, L.S., Chang, E.F., 2017. Intonational speech prosody encoding in the human auditory cortex. Science 357, 797–801.
Tedeschi, G., Trojsi, F., Tessitore, A., Corbo, D., Sagnelli, A., Paccone, A., D'Ambrosio, A., Piccirillo, G., Cirillo, M., Cirillo, S., Monsurro, M.R., Esposito, F., 2012. Interaction between aging and neurodegeneration in amyotrophic lateral sclerosis. Neurobiol. Aging 33, 886–898.
Terada, T., Miyata, J., Obi, T., Kubota, M., Yoshizumi, M., Yamazaki, K., Mizoguchi, K., Murai, T., 2017. Frontal assessment battery and frontal atrophy in amyotrophic lateral sclerosis. Brain Behav 7, e00707.
Thivard, L., Pradat, P.F., Lehericy, S., Lacomblez, L., Dormont, D., Chiras, J., Benali, H., Meininger, V., 2007. Diffusion tensor imaging and voxel based morphometry study in amyotrophic lateral sclerosis: relationships with motor disability. J. Neurol. Neurosurg. Psychiatry 78, 889–892.
Thorns, J., Jansma, H., Peschel, T., Grosskreutz, J., Mohammadi, B., Dengler, R., Munte, T.F., 2013. Extent of cortical involvement in amyotrophic lateral sclerosis–an analysis based on cortical thickness. BMC Neurol. 13, 148.
Tsermentseli, S., Leigh, P.N., Goldstein, L.H., 2012. The anatomy of cognitive impairment in amyotrophic lateral sclerosis: more than frontal lobe dysfunction. Cortex 48, 166–182.
Tsujimoto, M., Senda, J., Ishihara, T., Niimi, Y., Kawai, Y., Atsuta, N., Watanabe, H., Tanaka, F., Naganawa, S., Sobue, G., 2011. Behavioral changes in early ALS correlate with voxel-based morphometry and diffusion tensor imaging. J. Neurol. Sci. 307, 34–40.
Turner, M.R., Kiernan, M.C., 2012. Does interneuronal dysfunction contribute to neurodegeneration in amyotrophic lateral sclerosis? Amyotroph. Lateral Scler. 13, 245–250.
Turner, M.R., Hammers, A., Al-Chalabi, A., Shaw, C.E., Andersen, P.M., Brooks, D.J., Leigh, P.N., 2005. Distinct cerebral lesions in sporadic and 'D90A' SOD1 ALS: studies with [11C]flumazenil PET. Brain 128, 1323–1329.
Tzourio-Mazoyer, N., Landeau, B., Papathanassiou, D., Crivello, F., Etard, O., Delcroix, N., Mazoyer, B., Joliot, M., 2002. Automated anatomical labeling of activations in SPM using a macroscopic anatomical parcellation of the MNI MRI single-subject brain. NeuroImage 15, 273–289.
van der Hulst, E.J., Bak, T.H., Abrahams, S., 2015. Impaired affective and cognitive theory of mind and behavioural change in amyotrophic lateral sclerosis. J. Neurol. Neurosurg. Psychiatry 86, 1208–1215.
Vergani, F., Lacerda, L., Martino, J., Attems, J., Morris, C., Mitchell, P., Thiebaut De Schotten, M., Dell'Acqua, F., 2014. White matter connections of the supplementary motor area in humans. J. Neurol. Neurosurg. Psychiatry 85, 1377–1385.
Verma, G., Woo, J.H., Chawla, S., Wang, S., Sheriff, S., Elman, L.B., McCluskey, L.F., Grossman, M., Melhem, E.R., Maudsley, A.A., Poptani, H., 2013. Whole-brain analysis of amyotrophic lateral sclerosis by using echo-planar spectroscopic imaging. Radiology 267, 851–857.
Verstraete, E., Veldink, J.H., Mandl, R.C., van den Berg, L.H., van den Heuvel, M.P., 2011. Impaired structural motor connectome in amyotrophic lateral sclerosis. PLoS One 6, e24239.
Verstraete, E., Veldink, J.H., Hendrikse, J., Schelhaas, H.J., van den Heuvel, M.P., van den Berg, L.H., 2012. Structural MRI reveals cortical thinning in amyotrophic lateral sclerosis. J. Neurol. Neurosurg. Psychiatry 83, 383–388.
Verstraete, E., Veldink, J.H., van den Berg, L.H., van den Heuvel, M.P., 2014. Structural brain network imaging shows expanding disconnection of the motor system in amyotrophic lateral sclerosis. Hum. Brain Mapp. 35, 1351–1361.
Walhout, R., Westeneng, H.J., Verstraete, E., Hendrikse, J., Veldink, J.H., van den Heuvel, M.P., van den Berg, L.H., 2015. Cortical thickness in ALS: towards a marker for upper motor neuron involvement. J. Neurol. Neurosurg. Psychiatry 86, 288–294.
Westphal, A.J., Wang, S., Rissman, J., 2017. Episodic memory retrieval benefits from a less modular brain network organization. J. Neurosci. 37, 3523–3531.
Yao, Z., Zhang, Y., Lin, L., Zhou, Y., Xu, C., Jiang, T., Alzheimer's Disease Neuroimaging, I, 2010. Abnormal cortical networks in mild cognitive impairment and Alzheimer's disease. PLoS Comput. Biol. 6, e1001006.
Zhang, J., Wang, J., Wu, Q., Kuang, W., Huang, X., He, Y., Gong, Q., 2011. Disrupted brain connectivity networks in drug-naive, first-episode major depressive disorder. Biol. Psychiatry 70, 334–342.
Zhang, Y., Lin, L., Lin, C.P., Zhou, Y., Chou, K.H., Lo, C.Y., Su, T.P., Jiang, T., 2012. Abnormal topological organization of structural brain networks in schizophrenia. Schizophr. Res. 141, 109–118.
Zhang, J., Ji, B., Hu, J., Zhou, C., Li, L., Li, Z., Huang, X., Hu, X., 2017. Aberrant interhemispheric homotopic functional and structural connectivity in amyotrophic lateral sclerosis. J. Neurol. Neurosurg. Psychiatry 88, 369–370.
Zhou, C., Hu, X., Hu, J., Liang, M., Yin, X., Chen, L., Zhang, J., Wang, J., 2016. Altered brain network in amyotrophic lateral sclerosis: a resting graph theory-based network study at voxel-wise level. Front. Neurosci. 10, 204.
Zimmerman, E.K., Eslinger, P.J., Simmons, Z., Barrett, A.M., 2007. Emotional perception deficits in amyotrophic lateral sclerosis. Cogn. Behav. Neurol. 20, 79–82.